Effects of the Safety Factor on Ion Temperature Gradient Modes

A.K. Wang 1), J.Q. Dong 1), H. Sanuki 2), and K.Itoh 2)

1) Southwestern Institute of Physics, Chengdu, P.R. China
2) National Institute for Fusion Science, Toki, Japan
e-mail contact of main author: akwang@swip.ac.cn

Abstract: A model for the ion temperature gradient (ITG) driven instability is derived from Braginskii magnetohydrodynamic equations of ions. The safety factor q in a toroidal plasma is introduced into the model through the current density $\mathbf{J}_{//}$. The effects of q or $\mathbf{J}_{//}$ on both the ITG instability in $k_\perp$ and $k_{//}$ spectra and the critical stability thresholds are studied. It is shown that the current density $\mathbf{J}_{//}$ or the safety factor q plays an important role in stabilizing the ITG instability.

In the previous models [1, 2] for the ion temperature gradient (ITG) driven instability, the safety factor $q(r)$ is introduced into the model through the wavenumber or relative derivative, such as $k_\theta = lq(r)/r$ and $\nabla_{//} = ik_{//} = (Rq)^{-1}\partial/\partial\theta$. Since the safety factor does not directly stem from the current density, it cannot fully and realistically describe the roles of the current density or safety factor in the ITG mode stability. Hence, in this work we directly introduce the safety factor into the present model equations from the parallel current density and study the dependence of ITG mode stability on the current density or safety factor. In the present model, an important physical quantity, $\omega_J = 0.71\mathbf{k}\cdot(\mathbf{V}_{i//} - \mathbf{V}_{e//}) = 0.71(en_e)^{-1}\mathbf{k}\cdot\mathbf{J}_{//}$, involves the scalar product of the wave vector $\mathbf{k}$ and the relative motion of ion and electron fluid velocity ($\mathbf{V}_i - \mathbf{V}_e$), or equivalently, that of the wave vector $\mathbf{k}$ and the current density $\mathbf{J}_{//}$, and is expressed as [3]

$$\omega_J \begin{cases} = 0.71q\varepsilon^{-1}k_{//}(V_{*pe} - V_{*pi}) , & \text{for the limiting case of } k_\perp = 0, \\ = b_q(\omega_{*pe} - \omega_{*pi}), & \text{for a finite value of } k_\perp, \end{cases} \tag{1}$$

where $b_q = 0.71q\varepsilon^{-1}(k_{//}/k_\perp)$, $\omega_{*pe} = (1+\eta_e)\omega_{*e}$, and $\omega_{*pi} = (1+\eta_i)\omega_{*i}$. ω_J, including the parallel current density or the safety factor, will be incorporated into the following model equation.

From the Braginskii magnetohydrodynamic equations of ions [4] and the adiabatic electron response $\delta n_e/n_e = e\delta\phi/T_e$ along with quasi-neutrality $\delta n_e/n_e = \delta n_i/n_i$, we derive the dispersion relation for the ITG instability

$$[(\omega_{Di} - \omega_{*i} + b_i\Omega)(\Omega + \omega_{*pi} - \omega_J - 10\omega_{Di}/3) + \omega_{Di}(5\omega_{Di}/3 - \omega_{*pi} + 5b_i\Omega/3)]$$
$$= \tau[(\Omega + \omega_{*pi})(\Omega + \omega_{*pi} - \omega_J - 10\omega_{Di}/3) + 5\omega_{Di}^2/3], \tag{2}$$

where $\Omega = \Omega_r + i\gamma$, $b_i = -(k_\perp\rho_i)^2$, $\tau = T_i/Z_{eff}T_e$, and ω_J is given by Eq. (1). From Eqs (1) and (2), we see that ω_J describes the effects of $\mathbf{J}_{//}$ or q on the ITG instability. In the limiting case of $k_\perp = 0$, the solution of Eq. (2) for Ω is a stable mode

$$\Omega = \omega_J = 0.71q\varepsilon^{-1}k_{//}(V_{*pe} - V_{*pi}) . \tag{3}$$

When $k_\perp$ is finite, we get the unstable solution of Eq. (2) after all frequencies are normalized

to ω_{*e}

$$\Omega / \omega_{*e} = (\Omega_r + i\gamma) / \omega_{*e} = (\omega_r - \mathbf{k} \cdot \mathbf{V}_i + i\gamma) / \omega_{*e}, \tag{4}$$

where

$$2\frac{\Omega_r}{\omega_{*e}} = (1 + \tau / A_2 + b_q)\tau(1 + \eta_i) + b_q(1 + \eta_e) - 10\tau\varepsilon_n(1 + \tau / A_2)/3 + \tau(1 - 2\varepsilon_n)/A_2, \tag{5}$$

$$2\gamma / \omega_{*e} = [4(A_1 / A_2) - (2\Omega_r / \omega_{*e})^2]^{1/2}, \tag{6}$$

with

$$A_1 = (1 + b_q)\tau^3(1 + \eta_i)^2 + [b_q(1 + \eta_e) + (1 + b_q)(1 - 2\varepsilon_n) + (6 - 20\tau)\varepsilon_n / 3]\tau^2$$

$$\times (1 + \eta_i) + b_q(1 + \eta_e)\tau(1 - 2\varepsilon_n) + 20\tau^2\varepsilon_n(\tau\varepsilon_n + \varepsilon_n - 1)/3, \tag{7}$$

$$A_2 = \tau - b_i, \text{ and } \varepsilon_n = -(d\ln n / dr)/R.$$

If $k_{//} = 0$, Eqs (4–6) give an unstable mode without the q or $\mathbf{J}_{//}$ effect. For finite values of $k_\perp$ and $k_{//}$, the term b_q in Eqs (4–6) or ω_J describes the interaction between the unstable mode and the stable one ($\Omega = \omega_J$), which is the essence of the q or $\mathbf{J}_{//}$ effect. Such a function of ω_J is similar to the $\mathbf{E} \times \mathbf{B}$ shearing rate $\omega_{E \times B}$ [5], which can lead
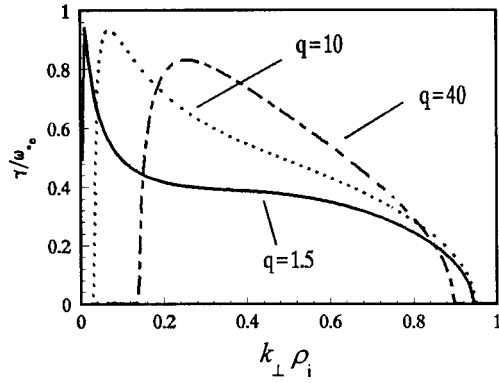

Fig. 1. γ / ω_{*e} *versus* $k_\perp \rho_i$ *for* $q = 1.5$, *10, and 40 when* $k_{//}\rho_i = 0.001$, $\varepsilon_n = 0.2$, $\tau = 1$, $\varepsilon = 0.2$, $\eta_e = 0$, *and* $\eta_i = 1.5$.
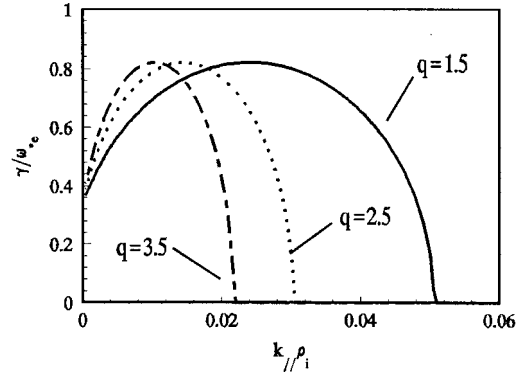
Fig. 2. γ / ω_{*e} *versus* $k_{//}\rho_i$ *for* $q = 1.5$, *2.5, and 3.5 when* $k_\perp \rho_i = 0.3$. *The other parameters are the same as in Fig. 1.*

to the coupling between the unstable mode and stable one. In Fig. 1, we show the growth rate γ / ω_{*e} versus $k_\perp \rho_i$ for different q values. The long wavelength instabilities in the $k_\perp$ spectrum are suppressed by the q or $\mathbf{J}_{//}$ effect, and the short wavelength instabilities ($k_\perp \rho_i \geq 0.92$) are suppressed by the finite Larmor radius effect. In addition, the q or $\mathbf{J}_{//}$ effect also suppresses the instabilities with larger wavenumber $k_{//}$, as shown in Fig. 2. The growth rate versus $k_\perp \rho_i$ is shown in Fig. 3 for different values of ε_n. When ε_n is very small, there are two discrete unstable regions in the perpendicular wavenumber spectrum. One is in the long wavelength region, $k_\perp \rho_i \sim 10^{-2}$ or $< 10^{-2}$. Another is in the short wavelength region, $k_\perp \rho_i \sim 0.3$ to 0.8. When ε_n is large enough, however, the instabilities in the short wavelength region are suppressed.

Setting the growth rate $\gamma = 0$ from Eq. (6), we can obtain the critical stability threshold equation of the ITG mode,
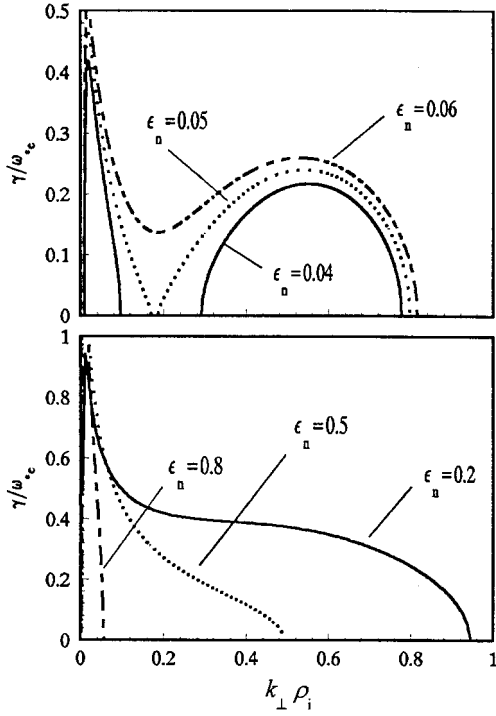
Fig. 3. Normalized growth rate versus $k_\perp \rho_i$ for different ε_n when $q = 1.5$ and $k_\perp \rho_i = 0.3$. The other parameters are the same as in Fig. 1
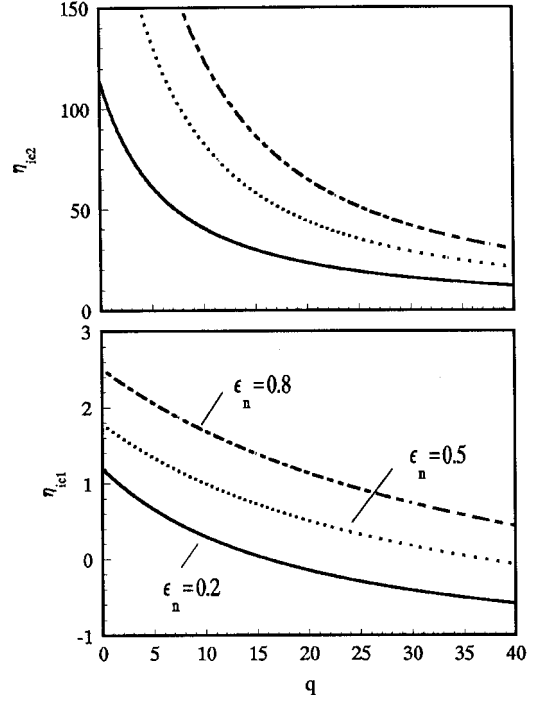
Fig. 4. η_{ic1} and η_{ic2} versus q for $\varepsilon_n = 0.2$, 0.5, and 0.8 when $k_\perp \rho_i = 0.3$. The other parameters are the same as in Fig. 1.

$$4A_1 / (\tau - b_i) - (2\Omega_r / \omega_{*e})^2 = 0. \tag{8}$$

This is a quadratic equation in η_i and q. Hence, in the present model, there are two stability thresholds for η_i and q, i.e. η_{ic1} and η_{ic2}, and q_{c1} and q_{c2} (generally $\eta_{ic1} \ll \eta_{ic2}$ and $q_{c1} \ll q_{c2}$). As a result, each of η_i and q has two stable parameter regimes. They are, respectively, $\eta_i \leq \eta_{ic1}$ and $\eta_i \geq \eta_{ic2}$, and $q \leq q_{c1}$ and $q \geq q_{c2}$. Correspondingly, each of η_i and q has an unstable parameter regime between the two stable regimes, i.e. $\eta_{ic1} < \eta_i < \eta_{ic2}$ and $q_{c1} < q < q_{c2}$. In order to study the critical stability thresholds of η_i, we substitute Eq. (7) into Eq. (8) and rewrite Eq. (8) as

$$y_2 (1 + \eta_i)^2 + y_1 (1 + \eta_i) + y_0 = 0, \tag{9a}$$

where

$$y_2 = [2\tau - b_i + b_q (\tau - b_i)]^2 \tau^2 - 4(\tau - b_i)(1 + b_q)\tau^3, \tag{9b}$$

$$y_1 = 2\tau [2\tau - b_i + b_q (\tau - b_i)][b_q (\tau - b_i)(1 + \eta_e) - 10\tau\varepsilon_n (2\tau - b_i)/3$$
$$+ \tau(1 - 2\varepsilon_n)] - 4(\tau - b_i)[b_q (1 + \eta_e) + (1 + b_q)(1 - 2\varepsilon_n) \tag{9c}$$
$$+ 2\varepsilon_n (3 - 10\tau)/3]\tau^2,$$

$$y_0 = [b_q(\tau - b_i)(1+\eta_e) - 10\tau\varepsilon_n(2\tau - b_i)/3 + \tau(1-2\varepsilon_n)]^2$$

$$- 4(\tau - b_i)[b_q(1+\eta_e)\tau(1-2\varepsilon_n) + 20\tau^2\varepsilon_n(\tau\varepsilon_n + \varepsilon_n - 1)/3]. \qquad (9d)$$

Thus, the two thresholds of η_i for the critical stability of the ITG mode are, respectively,

$$\eta_{ic1} = (2y_2)^{-1}[-y_1 - 2y_2 - (y_1^2 - 4y_0y_2)^{1/2}], \qquad (10a)$$

$$\eta_{ic2} = (2y_2)^{-1}[-y_1 - 2y_2 + (y_1^2 - 4y_0y_2)^{1/2}]. \qquad (10b)$$

Here, both η_{ic1} and η_{ic2} decrease with the increase of the safety factor q. When q is large enough, η_{ic1} goes through zero and then is negative. In this case, however, η_{ic2} reduces from over one hundred to the typical η_i parameter regime of tokamaks, i.e. $0 \le \eta_{ic2} < 10$, as is shown in Fig. 4. It is interesting that, under the specific condition of the parameters, i.e. $y_1^2 = 4y_0y_2$, $\eta_{ic1} = \eta_{ic2}$. That is, the unstable regime $\eta_{ic1} < \eta_i < \eta_{ic2}$ vanishes and thus the mode is stable without any η_i threshold. Here it should be pointed out that we have not found a typical parameter regime of tokamaks in which q, ε_n, τ, and ε, independently of each other, satisfy the condition. Similarly, Eq. (8) can be rewritten as

$$z_2q^2 + z_1q + z_0 = 0, \qquad (11a)$$

where

$$z_2 = (0.71\varepsilon^{-1}k_{//}/k_{\perp})^2(\tau - b_i)[\tau(1+\eta_i) + (1+\eta_e)]^2, \qquad (11b)$$

$$z_1 = 1.42\varepsilon^{-1}(k_{//}/k_{\perp})[\tau(1+\eta_i) + (1+\eta_e)][(2\tau - b_i)\tau(1+\eta_i) + \tau(1-2\varepsilon_n)$$

$$- 10\tau\varepsilon_n(2\tau - b_i)/3] - 2.84\varepsilon^{-1}(k_{//}/k_{\perp})[\tau^3(1+\eta_i)^2 + \tau^2(1+\eta_i)(1+\eta_e) \qquad (11c)$$

$$+ \tau^2(1+\eta_i)(1-2\varepsilon_n) + \tau(1+\eta_e)(1-2\varepsilon_n)],$$

$$z_0 = [(2\tau - b_i)\tau(1+\eta_i) + \tau(1-2\varepsilon_n) - 10\tau\varepsilon_n(2\tau - b_i)/3]^2 - 4$$

$$\times [(1+\eta_i)^2\tau^3 + (1+\eta_i)\tau^2\varepsilon_n(6-20\tau)/3 + (1+\eta_i)\tau^2(1-2\varepsilon_n) \qquad (11d)$$

$$20\tau^2\varepsilon_n(\tau\varepsilon_n + \varepsilon_n - 1)/3].$$

Then we obtain the two thresholds of q, which are, respectively,

$$q_{c1} = (2z_2)^{-1}[-z_1 - (z_1^2 - 4z_0z_2)^{1/2}], \qquad (12a)$$

$$q_{c2} = (2z_2)^{-1}[-z_1 + (z_1^2 - 4z_0z_2)^{1/2}]. \qquad (12b)$$

In particular, when the parameters satisfy the following condition
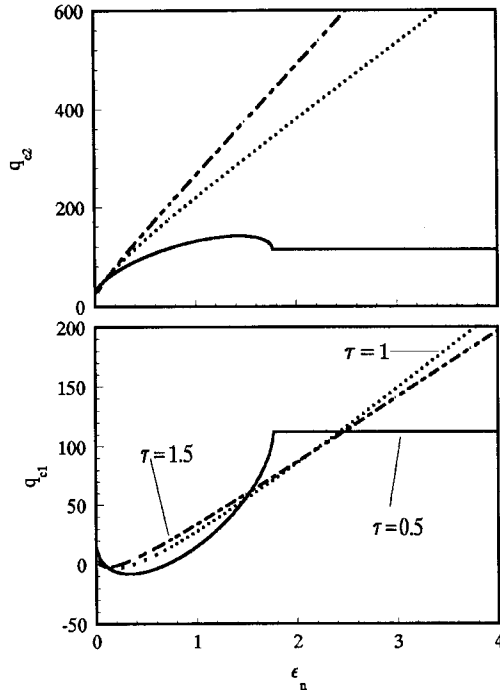
$$z_1^2 = 4z_0z_2, \qquad (13)$$

Fig. 5. q_{c1} *and* q_{c2} *versus* ε_n *for* $\tau = 0.5, 1, and$
1.5 when $k_\perp \rho_i = 0.3$. *The other parameters are the same as in Fig. 1.*

$q_{c1} = q_{c2}$. Thus, the unstable q parameter regime vanishes and the mode is stable for any value of q. This situation is shown in Fig. 5, where $q_{c1} = q_{c2} = 115$ when $\varepsilon_n \geq 1.8$. Usually ion internal thermal transport barriers are observed in reversed shear plasmas. However, there are regimes, such as the high-β_p H-mode [6], for which the profile of reversed shear is not present but for which an ion core transport barrier certainly forms. The present theoretical result should be a possible scenario to explain the experiment of the high-β_p H-mode.

In summary, the parallel current density or the safety factor is introduced into the present model. Its effects are to suppress both the longer wavelength mode in the $k_\perp$ spectrum and the shorter wavelength mode in the $k_{//}$ spectrum. In addition, it is shown that there exist two critical stability thresholds of both η_i and q. They correspond to two stable regimes and one unstable regime between the two stable ones. The first stable regime is in the typical parameter range of present day tokamaks.

ACKNOWLEDGEMENTS

REFERENCES

[1] W. Horton, Rev. Mod. Phys. **71** (1999) 735.
[2] J. Weiland, Collective Modes in Inhomogeneous Plasma: Kinetic and Advanced Fluid Theory, IOP Publishing, Bristol (2000) 115–142.
[3] A.K. Wang, J.Q. Dong, W.X. Qu, X.M. Qiu, Phys. Plasmas **9** (2002) 748.
[4] S.I. Braginskii, Reviews of Plasma Physics, Consultants Bureau, New York (1965) 205.
[5] K.H. Burrell, Phys. Plasmas **4** (1997) 1499.
[6] Y. Koide et al., Phys. Rev. Lett. **72** (1994) 3662.